Journal of Reinforced Plastics and Composites

http://jrp.sagepub.com

Interlaminar Shear Stresses in Composite Laminates Due to Static Indentation

Bhavani V. Sankar

Journal of Reinforced Plastics and Composites 1989; 8; 458
DOI: 10.1177/073168448900800504

The online version of this article can be found at:
http://jrp.sagepub.com/cgi/content/abstract/8/5/458

Published by:
SAGE
http://www.sagepublications.com

Interlaminar Shear Stresses in Composite Laminates Due to Static Indentation

BHAVANI V. SANKAR
Department of Aerospace Engineering
Mechanics & Engineering Science
University of Florida
Gainesville, FL 32611

ABSTRACT: Finite difference method is used to analyze the axisymmetric problem of smooth contact between a rigid indenter and a laminated circular plate clamped at the edges. The plate is assumed to be made up of transversely isotropic layers. The numerical study shows that interlaminar shear stresses in the vicinity of contact are much different from the laminate plate theory solutions, and that low-modulus surface layers and interlayers can help in reducing the maximum interlaminar shear stresses due to static indentation.

KEY WORDS: composite laminates, impact damage, indentation damage, interlaminar shear stresses, interleaving.

1. INTRODUCTION

DURING THE PAST several years considerable amount of research has been done in understanding low-energy impact response and damage in composite structures. Current efforts in this area are focused on developing simple design procedures so that the impact damage can also be taken into account in the design of composite structures. In this regard a thorough understanding of the detailed stress field in various types of laminates under various impact conditions has become crucial. Recent studies [1–4] have shown that static indentation tests may provide useful information about the failure mechanisms and failure loads for impacts by a large mass at low velocities, e.g., 1–10 kg at 1–3 m/s. Further static indentation tests are inexpensive and well suited for small samples of material systems that are in development stage. It has also been found that interleaving the laminates with PEEK layers or adhesive layers will reduce the extent of delamination due to impact [5]. But, a systematic and scientific study is needed to estimate the optimum location and extent of the interleave materials that will be effective in arresting delamination propagation.

This paper was presented at the Third Technical Conference of the American Society for Composites.

0731-6844/89/05 0458-14 $4.50/0

Laminate theories are not adequate in describing the stresses due to indentation or for that matter impact. Figure 1 shows the load-deflection diagram of two different 32 layer quasi-isotropic graphite/epoxy laminated plates indented by indenters with diameters 6.25 mm and 25.4 mm. In these diagrams the nonlinear portion due to local indentation is not shown. The dimensions of the plate are 125 × 125 mm and 70 × 70 mm respectively. According to the laminate theory the failure load of 70-mm plates should be about 1.8 times ($\cong 125/70$) that of 125-mm plates irrespective of indenter diameter. But, it may be seen from Figure 1 that the failure loads strongly depend on the indenter diameters rather than on the extent of laminate. One can also notice the apparent increase in stiffness for the case of larger indenter. This suggests that three-dimensional analysis is essential in the understanding of failure due to indentation. Further experiments are under way to characterize damage in composite laminates due to static indentation.

The present study will focus on the numerical analysis of interlaminar shear stresses in a composite laminate indented by a rigid indenter (see Figure 2). The plate is assumed to be circular, made up of transversely isotropic layers, and clamped at the boundary. Finite difference method is used to solve the elasticity equations in the inner region where local indentation effects will dominate. Laminated plate theory is used in the outer region away from the contact region. Displacements obtained from both solutions are matched at the transition boundary

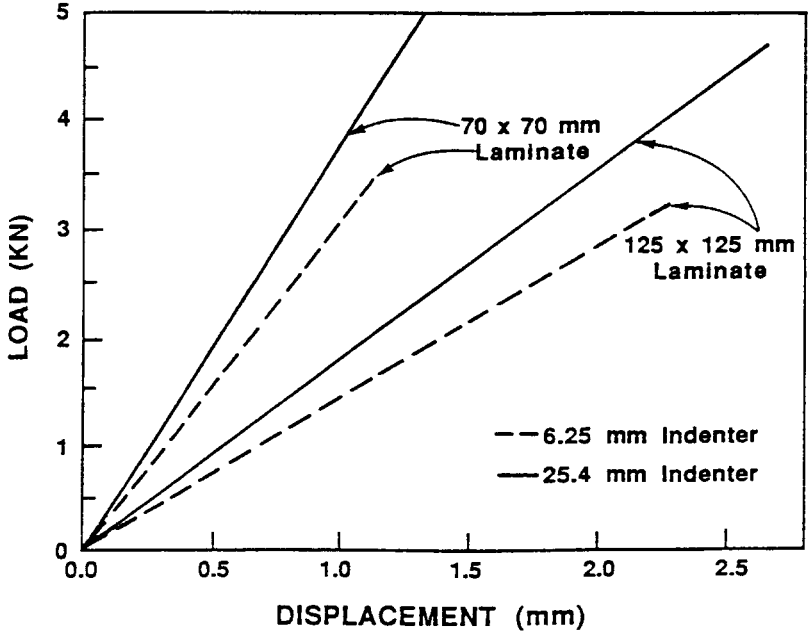

Figure 1. *Effect of plate dimensions and indenter diameter on failure load of graphite/epoxy plates.*

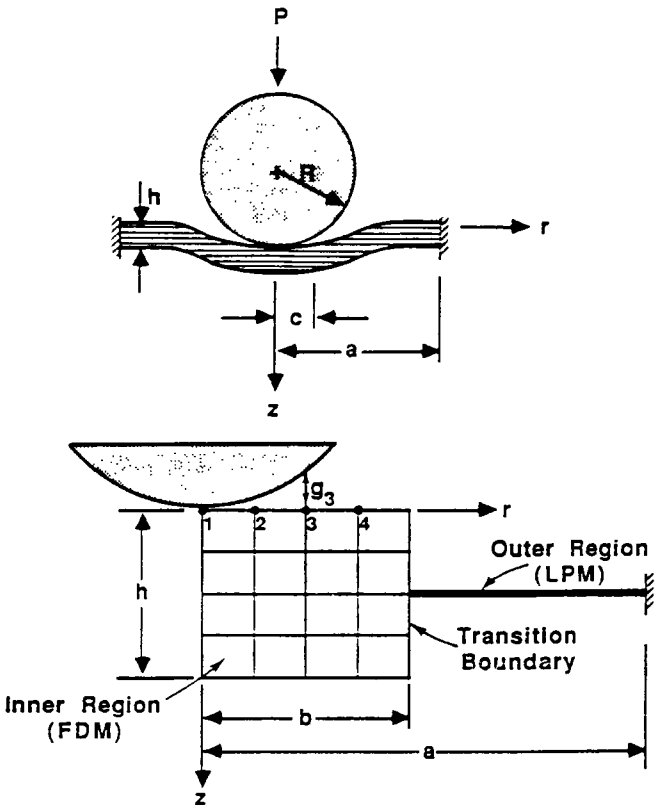

Figure 2. *Axisymmetric indentation of a composite laminate.*

between the inner and outer regions. The results presented are: contact stresses, variation of contact radius with contact force, and interlaminar shear stress distribution. The effects of a soft surface layer and an interlayer on the contact behavior and interlaminar shear stresses are discussed.

2. FINITE DIFFERENCE FORMULATION

Aboudi [6] has solved several 2-D and 3-D dynamic indentation problems using finite difference method. The equilibrium equations for axisymmetric problems are

$$C_{11}(u,rr + r^{-1}u,_r - r^{-2}u) + C_{44}u,_{zz} + (C_{13} + C_{44})w,_{rz} = 0 \qquad (1)$$

and

$$(C_{13} + C_{44})(u,_{rz} + r^{-1}u,z) + C_{44}(w,_{rr} + r^{-1}w,_r) + C_{33}w,_{zz} = 0 \qquad (2)$$

where u and w are displacements in the r and z directions respectively, and a comma denotes partial differentiation with respect to subscripted variables. The relation between the engineering elastic constants and the stiffness coefficients C_{ij}'s may be found in [7].

The finite difference approximation to Equations (1) and (2) are obtained by replacing all the partial derivatives by corresponding central differences, and applying them to all the interior points in each layer. On the top surface of the plate vertical displacements are imposed at points beneath the indenter, whereas normal stresses are made equal to zero at points outside the contact radius. Shear tractions are assumed to be zero on the entire top surface. Continuity of interlaminar shear and normal stresses is imposed at points on the interface between two layers. Normal and shear tractions vanish at points on the bottom surface of the plate. Forward and backward differences are used to compute z-derivatives in the stress terms on the top and bottom surfaces of any layer respectively. For points on the z-axis radial displacements are zero. Further a limiting process [6] has to be used to compute some of the r-derivatives at $r = 0$.

As will be described in Section 4 below, the finite difference method was used to solve the boundary value problem where w-displacements are prescribed over part of the top surface. Gauss-Seidel iteration was used to solve the set of linear equations in a computer with vector processing capability. The radial displacements at the transition boundary were obtained using the LPM (Laminated Plate Model) discussed in Section 3. The total load acting at the center of the plate was calculated from the FDM (Finite Difference Model) at the end of each Gauss-Seidel iteration. This force was applied as a central force in the LPM to compute the radial displacements at the transition boundary. Then the displacements were used as updated boundary conditions for the next iteration of FDM. The w-displacements at the transition boundary obtained from the LPM were not used, because they simply add to the rigid body displacement of the inner region, and do not affect the contact stresses or any other stress component for that matter.

3. LAMINATE PLATE THEORY FOR CIRCULAR PLATES

Laminate plate theory was used to calculate the radial displacements on the transition boundary. The differential equations of equilibrium for circular plates are [8]:

$$rN_{r,r} + (N_r - N_\theta) = 0 \tag{3}$$

$$rM_{r,r} + (M_r - M_\theta) = -Qr \tag{4}$$

where N_r and N_θ are the in-plane force resultants, M_r and M_θ are the moment resultants, and Q is the shear force resultant. The constitutive relations are

$$\begin{Bmatrix} N_r \\ N_\theta \end{Bmatrix} = \begin{bmatrix} A_{11} & A_{12} \\ A_{12} & A_{22} \end{bmatrix} \begin{Bmatrix} \epsilon_{rr} \\ \epsilon_{\theta\theta} \end{Bmatrix} + \begin{bmatrix} B_{11} & B_{12} \\ B_{12} & B_{22} \end{bmatrix} \begin{Bmatrix} \kappa_{rr} \\ \kappa_{\theta\theta} \end{Bmatrix} \tag{5}$$

and

$$\begin{Bmatrix} M_r \\ M_\theta \end{Bmatrix} = \begin{bmatrix} B_{11} & B_{12} \\ B_{12} & B_{22} \end{bmatrix} \begin{Bmatrix} \epsilon_{rr} \\ \epsilon_{\theta\theta} \end{Bmatrix} + \begin{bmatrix} D_{11} & D_{12} \\ D_{12} & D_{22} \end{bmatrix} \begin{Bmatrix} \varkappa_{rr} \\ \varkappa_{\theta\theta} \end{Bmatrix} \tag{6}$$

where the mid plane strains and curvatures are defined as $\epsilon_{rr} = du_0/dr$, $\epsilon_{\theta\theta} = u_0/r$, $\varkappa_{rr} = d\psi/dr$, $\varkappa_{\theta\theta} = \psi/r$, $\psi = dw_0/dr$, and u_0 and w_0 are the midplane radial and transverse displacements, respectively.

From Equations (3)–(6) one can derive a pair of coupled ordinary differential equations in $u_0(r)$ and $\psi(r)$. In these equations all the first and second derivatives were approximated by their corresponding central differences, and solved by using the Gauss-Seidel iterative procedure. For a centrally loaded clamped plate the boundary conditions are: $u_0(0) = 0$, $\psi(0) = 0$, $u_0(a) = 0$, $\psi(a) = 0$, and $Q = -P/(2\pi r)$, where P is the concentrated force at the center, and a is the plate radius. As discussed in the previous section we do not require w-displacements at the transition boundary for solving the contact problem. The radial displacements at the transition boundary, $r = b$, are computed as $u(b,z) = u_0(b) - z\psi(b)$.

4. A NUMERICAL ALGORITHM FOR THE CONTACT PROBLEM

The initial contact between the rigid indenter and the plate is assumed to occur at the central node. As the indenter is moved down, successive nodes come into contact with the indenter, and their boundary conditions are changed. In Reference [9] the contact problem was solved assuming the contact pressure as a superposition of several uniform loads acting over different radii. The unknowns in the contact stress distribution were solved from a set of linear algebraic equations obtained from the condition that the deformed surface of the plate beneath the indenter should conform to the shape of the indenter.

In the present method a slightly different approach is used. First several boundary value problems were solved, the boundary conditions for the ith problem being

$$w_k = 1, \quad 1 \leq k \leq i$$

and

$$\sigma_{zz} = 0, \quad k > i$$

where w_k is the w-displacement of the kth node on the top surface. The computed surface displacements w_j are denoted by f_j^i, which are actually influence functions. For example f_j^i is the w-displacement of the jth node due to unit displacements at Nodes 1 through i. The stress field $\{\sigma^i\}$ was also calculated at all points of interest.

Let the vertical gap between the ith node and the indenter at the beginning of contact be g_i. For a paraboloidal indenter $g_i = (i - 1)^2\Delta^2/(2R)$ where R is the

indenter radius of curvature, and Δ is the finite difference mesh size. The initial contact is at Node 1. Now we compute the amount of vertical displacement δ_1 required by the indenter to close the gap g_2 using the equation $\delta_1 - f_2^1\delta_1 = g_2$. After the indenter moves through a distance of δ_1, the gaps at other nodes would have changed. For example, current gap e_3 at the Node 3 will be given by $e_3 = g_3 - \delta_1(1 - f_3^1)$. In the next step the amount of indenter displacement δ_2 needed to close the gap e_3 is computed. In general the equation for the nth step is:

$$\delta_n = e_{n+1}/(1 - f_{n+1}^n)$$

where the current gap e_{n+1} at Node $n + 1$ is given by

$$e_{n+1} = g_{n+1} - \sum_i \delta_i(1 - f_{n+1}^i)$$

Once the δ's are calculated, the stress field due to indentation can be calculated from

$$\{\sigma\} = \sum_i \delta_i\{\sigma^i\}$$

The contact force is obtained as

$$P = -2\pi \int_0^c \sigma_{zz}(r,0)r\,dr \tag{7}$$

where c is the contact radius. The integral in (7) has to be computed numerically using the σ_{zz} values at the contact nodes obtained from the FDM.

5. RESULTS AND DISCUSSION

In the numerical examples the plate diameter was assumed to be 50 mm and the thickness 2 mm. The diameter of the inner region modeled by elasticity equations was 10 mm. The inner region was modeled by a 100 × 40 mesh with uniform spacing. The indenter radius of curvature was 10 mm, and the computations were performed for a maximum contact radius of 1 mm.

The elastic constants of materials used in the numerical study are given in Table 1. Two different types of laminate configurations were studied (see Figure 3). In Configuration 1 (Laminates 1A, 1B and 1C) the layers are all isotropic. This example was chosen to bring out the important features of the laminate contact problem, and the effect of mismatch of elastic constants of adjacent layers. Configuration 2 (Laminates 2A, 2B and 2C) represents more realistic composite material systems. The properties of Material 3 are approximately equal to that of a four ply graphite/epoxy quasi-isotropic laminate idealized as a homogeneous transversely isotropic layer. Properties of Material 4 are obtained by similar idealization of glass/epoxy layers. Material 5 is assumed as an epoxy-resin.

Table 1. Elastic constants of materials used in numerical examples.

Material	E_r, GPa	E_z, GPa	G_{rz}, GPa	ν_{rz}	$\nu_{r\theta}$
1	200	200	80.0	0.25	0.25
2	20	20	8.0	0.25	0.25
3	50	7	3.8	0.285	0.265
4	20	8	3.6	0.270	0.255
5	3	3	1.1	0.350	0.350

Results for Configuration 1 are presented in Figures 4 through 7. In these figures the legends Homogeneous, Surface Layer and Interleaf represent the lay-ups shown in Figure 3(a). For small contact radii ($c < 0.125$ h) the contact stress distribution in all the three laminates was Hertzian. For larger contact radii the deviation from elliptical distribution was significant. From Figure 4 it may be seen that the contact stresses in the homogeneous plate are still Hertzian, whereas there is considerable deviation in the other two plates. In the presence of a soft surface layer on top, the contact stresses peak at the center. When the soft layer is used as an interleaf the contact stresses are almost uniform except at the periphery of the contact circle, and the maximum contact stress at the center is reduced by 20%. Such details of contact stresses are important, because their effect on the stress field is significant.

The variation of contact force with the contact radius is presented in Figure 5. The two extreme curves represent the homogenous plates made up of materials 1 and 2. In the homogeneous plates the contact force is proportional to c^3 as in an isotropic half-space [10]. In Laminates 1B and 1C, for small contact lengths the contact behavior is controlled by the properties of the layer in contact with the indenter. As the contact force is increased the layer beneath the surface layer influences the extent of contact for a given contact force. The contact force for a

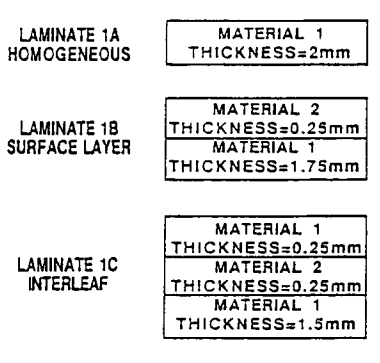

Figure 3a. Configuration 1

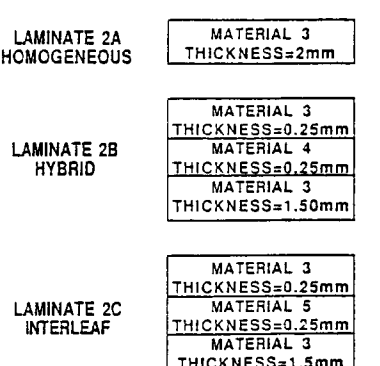

Figure 3b. Configuration 2

Figure 3. *Laminate configurations used in numerical studies.*

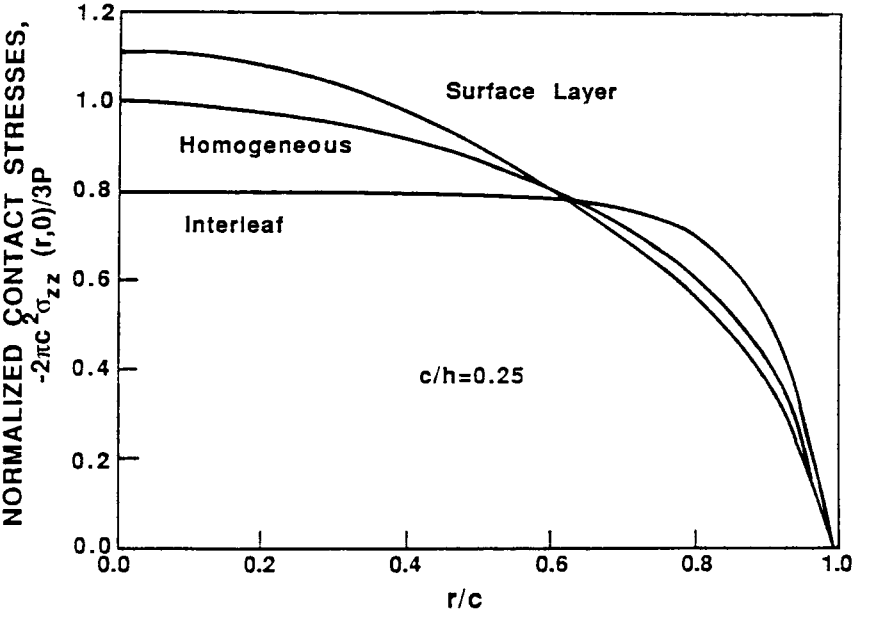

Figure 4. *Contact stresses in composite laminates (configuration 1).*

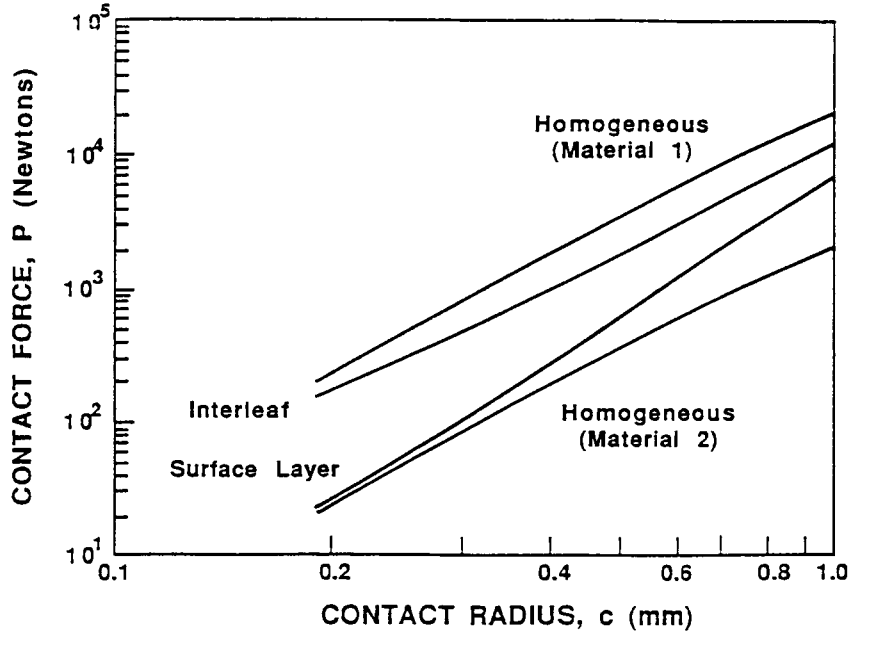

Figure 5. *Contact force-contact radius relations for configuration 1.*

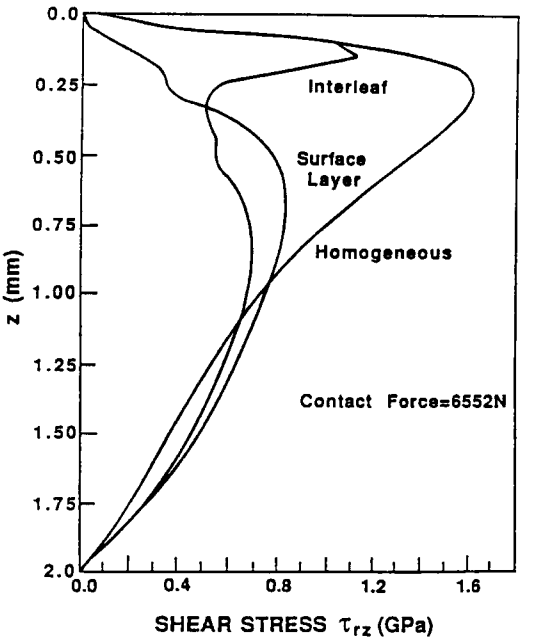

Figure 6. *Example of interlaminar shear stress distribution for configuration 1.*

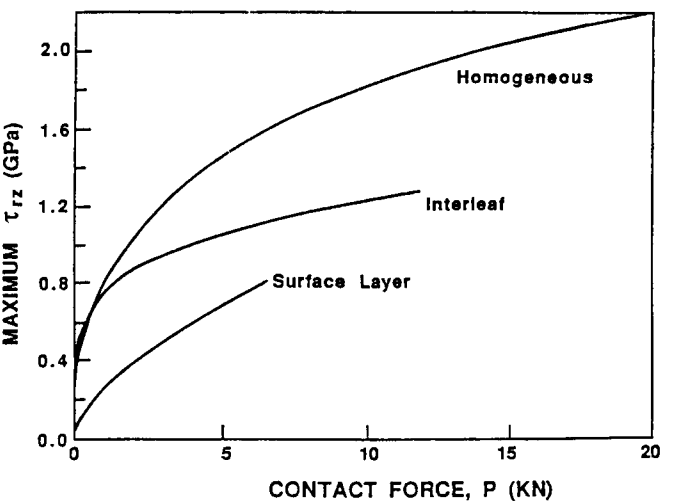

Figure 7. *Maximum interlaminar shear stresses-contact force relationship for configuration 1.*

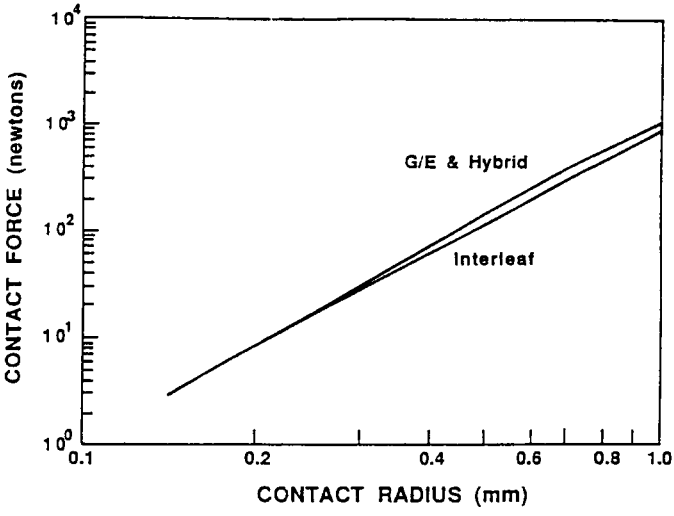

Figure 8. *Contact force-contact radius relations for configuration 2.*

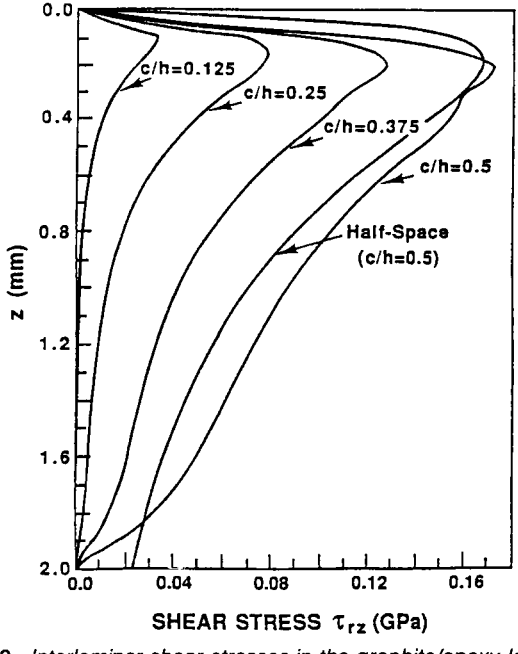

Figure 9. *Interlaminar shear stresses in the graphite/epoxy laminate.*

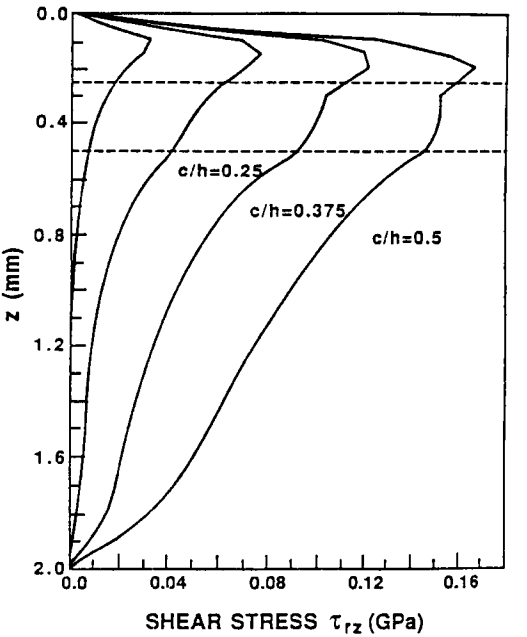

Figure 10. *Interlaminar shear stresses in the hydrid laminate.*

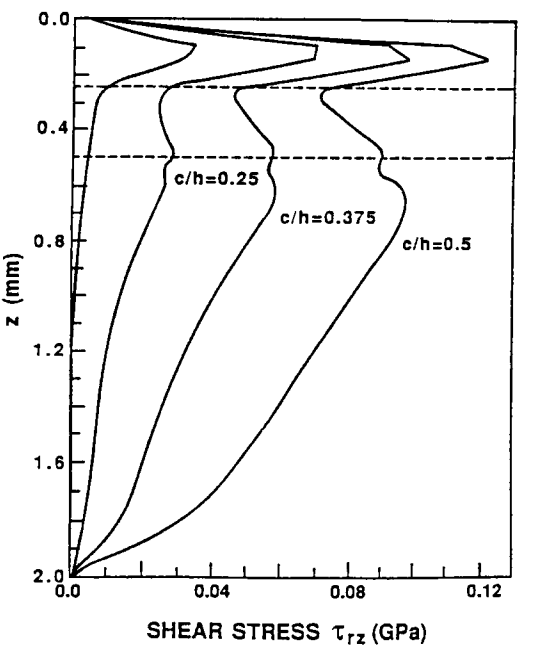

Figure 11. *Interlaminar shear stresses in the interleaved laminate.*

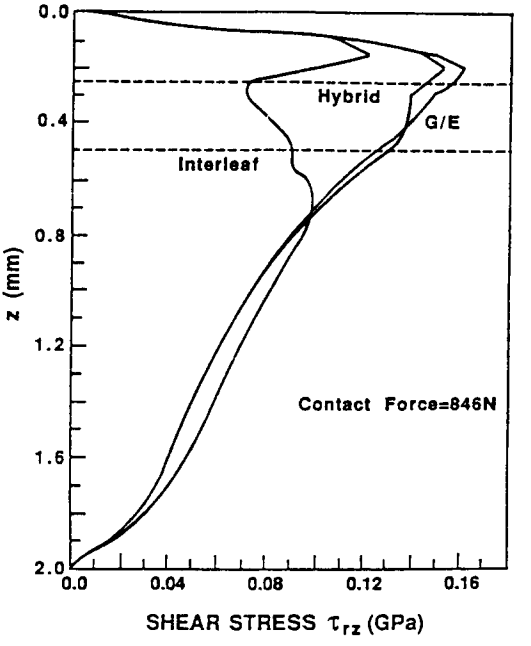

Figure 12. *Comparison of interlaminar shear distribution for configuration 2.*

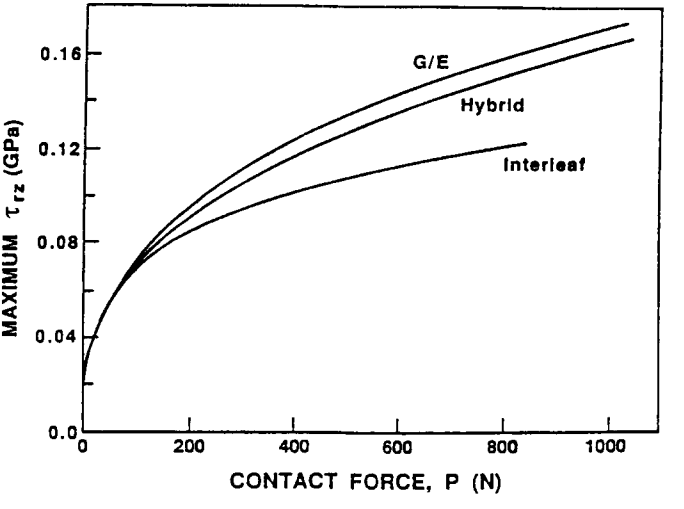

Figure 13. *Maximum interlaminar shear stress-contact force relationship for configuration 2.*

given contact radius c is bounded by the corresponding values for Material 1 and 2. If one desires to model the contact force-contact radius relation by a power law of type $P = kc^n$, then the exponent n will be greater or less than 3 depending on whether the soft layer is used as a surface layer or interlayer.

The interlaminar shear stress distribution in the three plates for a given contact force is shown in Figure 6. The stresses for each case are presented at a radius where the maximum shear stress occurs. It was found that the maximum shear stress occurs at a radius slightly less than the contact radius (between 0.9 c and 0.95 c). The effect of surface layer and interlayer in reducing the interlaminar shear is evident. The interlaminar shear in the homogenous case was found to be closely related to the half-space solution [11]. When the soft material is used as an interleaf the maximum shear stress is still in the top layer, and the shear stress in the interlayer is almost constant. When Material 2 is used as a surface layer, the location of maximum shear is pushed down. The variation of maximum interlaminar shear stress with respect to the contact force is presented in Figure 7. Once again one can see that the interlayer and surface layer have significant effect in reducing the maximum shear stress for a given contact force.

The results for Configuration 2 (Laminates 2A, 2B and 2C) are presented in Figures 8 through 13. In these figures the legends G/E, Hybrid and Interleaf represent the homogenous graphite/epoxy laminate, plate with an interlayer of glass/epoxy, and plate with an interlayer of epoxy resin respectively. The contact stresses in all the three plates were close to the Hertzian distribution, and the figures are not presented here. There is not much difference in the contact force-contact radius relations (Figure 8) also. This is because the top layers of all three plates are the same.

The interlaminar shear stress distribution in the three laminates for various contact radii are shown in Figures 9–11. The shear stresses in the homogeneous graphite/epoxy plate (Figure 9) were very similar to that in a transversely isotropic half-space [11]. In the presence of interleaves (Figures 10 and 11) the maximum interlaminar shear still occurs in the top layer, but it is considerably less than that in the homogeneous plate (cf. Figure 9). The same trend can be observed in Figure 12 where the shear stresses in all the three laminates due to a given contact force are presented. Figure 13 shows the variation of maximum interlaminar shear with the contact force. One may observe that interleaving with a soft layer can significantly reduce the maximum interlaminar shear stress.

The present numerical study shows that the interlaminar shear stresses in a composite laminate subjected to static indentation can be considerably reduced by interleaving with a layer of low modulus material such as epoxy resin. One should expect similar results with PEEK interleaf also. Experimental studies are underway to see if this could reduce the extent of damage during static indentation. The results can be extended, at least qualitatively, to low-velocity impact situations.

ACKNOWLEDGEMENTS

This study was initiated when the author was working at the Wright-Patterson Air Force Base Materials Laboratory under the subcontract RI-51542X through

the University of Dayton Research Institute. The author is grateful to Mr. T. M. Cordell and Dr. N. J. Pagano for many helpful discussions and encouragement. Partial support was provided by the NASA Langley Research Center Grant NAG-1-826. The support of Pittsburgh Supercomputer Center through the NSF Grant MSM 8708764 is also acknowledged.

REFERENCES

1. Sankar, B. V. "Low-Velocity Impact Response of Graphite-Epoxy Laminates," Final Report. Department of Engineering Sciences, University of Florida. WPAFB Contract F33615-84-C-5070 (September 1987).
2. Poe, C. C., Jr. "Simulated Impact Damage in a Thick Graphite/Epoxy Laminate Using Spherical Indenters," *Proceedings of the American Society for Composites: Third Technical Conference*. Lancaster, PA:Technomic Publishing Co., Inc. (1988).
3. Sjoblom, P. O., J. T. Hartness and T. M. Cordell. "On Low-Velocity Impact Testing of Composite Materials," *J. Composite Materials*, 22:30–52 (1988).
4. Elber, W. "Failure Mechanics in Low-Velocity Impacts on Thin Composite Plates," *NASA Technical Paper 2152* (1983).
5. Sun, C. T. and S. Rechak. "Effect of Adhesive Layers on Impact Damage in Composite Laminates," *ASTM STP 972* (1988).
6. Aboudi, J. "The Dynamic Contact Stresses Caused by the Impact of a Nonlinear Elastic Half-Space by an Axisymmetrical Projectile," *Comp. Methods App. Mech. Engineering*, 13:189–204 (1978).
7. Jones, R. M. *Mechanics of Composite Materials*. Washington, DC:Scripta Book Co. (1975).
8. Timoshenko, S. and S. Woinowsky-Krieger. *Theory of Plates and Shells*. New York, NY: McGraw-Hill Book Co. (1959).
9. Sankar, B. V. "Contact Law for Transversely Isotropic Materials," *Paper No. AIAA-85-0745*. Presented at the AIAA SDM Conference (1985).
10. Timoshenko, S. P. and J. N. Goodier. *Theory of Elasticity*. New York, NY:McGraw-Hill (1970).
11. Dahan, M. and J. Zarka. "Elastic Contact between a Sphere and a Semi Infinite Transversely Isotropic Body," *Int. J. Solids Structures*, 13:229–238 (1977).